Gradient Ascent Based Optimization for a Reconfigurable OTA Chamber

Matthew D. Arnold†, Rashid Mehmood†, Michael A. Jensen†, and Jon W. Wallace*

†Brigham Young University, Provo, UT, USA
E-mail: jensen@byu.edu

*Lafayette College, Easton, PA, USA
E-mail: wall@ieee.org

***Abstract*—A reconfigurable over-the-air chamber represents a reverberation chamber whose walls are lined with antennas that are terminated in reconfigurable impedances, allowing synthesis of a wide range of channel conditions for over-the-air testing of mobile wireless devices. While these chambers have potential for practical device testing, finding the right impedances to achieve the desired channel characteristics remains a challenging problem. This work explores the use of a simple gradient ascent optimization algorithm to determine the impedance states that achieve a specified spatial structure in the multipath, as characterized by the multipath power angular spectrum. The results highlight that the optimization is effective for synthesizing a desired power angular spectrum with a directive peak and a relatively low sidelobe level.**

I. Introduction

Over-the-air (OTA) testing allows the incorporation of the antennas while testing the communication performance of mobile wireless devices in realistic and repeatable propagation environments. Multi-probe anechoic chamber-based OTA testing [1], [2] allows the synthesis of arbitrary fading statistics coupled with flexible spatial channel characteristics experienced by the device under test (DUT), but unfortunately this method has a high associated cost. Reverberation chamber-based OTA testing, where the multipath environment is created inside a closed cavity and varied through mechanical *stirring* with moving paddles [3], offers a significantly reduced cost. However, this testing approach offers very limited control of the synthesis of arbitrary propagation environments.

The reconfigurable OTA chamber (ROTAC) has recently been proposed as a potential method for achieving reasonable cost and high flexibility in creating realistic propagation environments [4]. The ROTAC is effectively a reverberation chamber whose walls are lined with several antennas, a small number of which are used to excite the chamber and the remainder of which are terminated with reconfigurable impedance elements (REs) to control the reflections of waves from the walls. Recent work on the ROTAC has used both simulation models and hardware prototypes [4]–[6] based on patch and monopole antennas to demonstrate that the ROTAC can allow the generation of arbitrary fading statistics and spatial channel characteristics at the DUT.

Development of efficient algorithms for real-time optimization of RE impedances to generate a specific multipath environment inside the chamber remains an outstanding question. Unfortunately, the optimization problem is non-convex and nonlinear, and no direct closed form solution has yet been determined. Past work has therefore used either a random search or a genetic algorithm for optimization [4], [5], methods that are computationally expensive and unsuitable for real-time optimization in operational testing. This work explores the use of a simple gradient ascent optimization algorithm for this problem. Although different optimization goals can be considered, we have focused our attention on the control of the power angular spectrum (PAS) observed by the DUT, as our experience shows that this channel characteristic is generally more difficult to optimize than fading statistics. Results indicate that, even when the starting point is randomly selected, the gradient ascent algorithm can find reasonably good solutions with reduced computational burden.

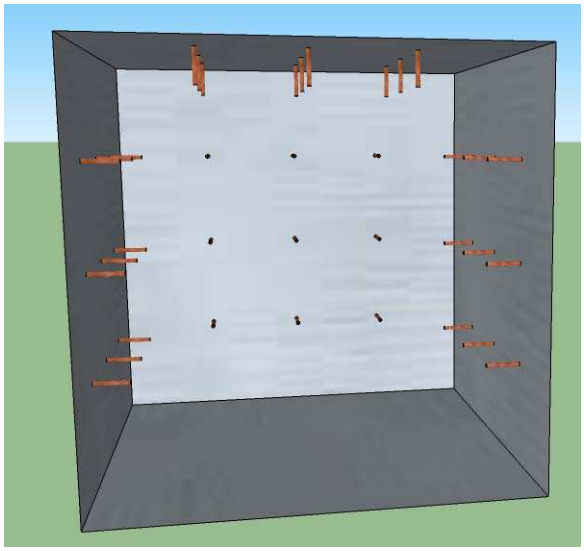

Fig. 1. Model for the ROTAC, where one side panel has been removed from the figure to allow visualization of the chamber interior.

II. Analysis

The ROTAC model considered in this analysis is a perfect electric conducting cube with a side length of 30.5 cm as shown in Figure 1. The top and four side walls of the chamber are equipped with a grid of 3×3 ports each of which is connected to a monopole antenna. In order to compute the fields inside the chamber for arbitrary RE states, we have used a hybrid approach that combines full-wave simulations conducted with the finite-difference time-domain (FDTD) method and network analysis to incorporate the changing RE

978-88-907018-7-0/17/$31.00 ©2017 IEEE

#1570318008

impedance values [4]. Specifically, for N antenna ports on the chamber walls, we conduct N FDTD simulations wherein one of the ports is excited with a unit source while all others are terminated with the system impedance $Z_0 = 50\Omega$. This allows computation of the chamber fields due to excitation from each port as well as the full S-parameter matrix for the chamber.

A. Optimization Goal

We assume that the lower right port on each side wall of the chamber is an excitation or *feed* port, while the remaining 8 ports on each wall and the 9 ports on the top are equipped with REs, meaning we have $N_{\mathrm{F}} = 4$ feed and $N_{\mathrm{R}} = 41$ RE ports. We partition the S-parameter matrix into the $N_{\mathrm{R}} \times N_{\mathrm{R}}$ matrix $\mathbf{S}_{\mathrm{RR}}$ relating the RE ports to each other and the $N_{\mathrm{R}} \times N_{\mathrm{F}}$ matrix $\mathbf{S}_{\mathrm{RF}}$ relating the feed to the RE ports. If $\mathbf{\Gamma}$ is the $N_{\mathrm{R}} \times N_{\mathrm{R}}$ diagonal matrix whose diagonal entries represent the reflection coefficients on the RE ports for the given RE state, then the electric field in a single polarization measured at the point $\mathbf{r}$ in the chamber can be expressed as [7]

$$e(\mathbf{r}) = \left[\mathbf{e}_{\mathrm{F}}^{\mathrm{T}}(\mathbf{r}) + \mathbf{e}_{\mathrm{R}}^{\mathrm{T}}(\mathbf{r})\mathbf{\Gamma}(\mathbf{I} - \mathbf{S}_{\mathrm{RR}}\mathbf{\Gamma})^{-1}\mathbf{S}_{\mathrm{RF}}\right]\mathbf{a}_{\mathrm{F}}, \quad (1)$$

where $\mathbf{e}_{\mathrm{F}}(\mathbf{r})$ and $\mathbf{e}_{\mathrm{R}}(\mathbf{r})$ are $N_{\mathrm{F}} \times 1$ and $N_{\mathrm{R}} \times 1$ vectors representing the field at $\mathbf{r}$ due to unit excitation on each of the feed and RE ports, respectively, $\{\cdot\}^{\mathrm{T}}$ is a transpose, and $\mathbf{a}_{\mathrm{F}}$ is the $N_{\mathrm{F}} \times 1$ vector containing the feed port excitations. In this work, we assume purely reactive REs that have no loss and a phase tunability in the range $[0°, 360°]$. Therefore, the ith diagonal entry of $\mathbf{\Gamma}$ can be expressed as $\Gamma_{ii} = e^{j\theta_i}$, where θ_i is the phase of the reflection coefficient of the ith RE.

To compute the realized PAS for a given RE state (represented by $\mathbf{\Gamma}$), we apply the Bartlett beamformer to the signals received by a uniform circular array (UCA) with a radius of 6 cm and $N_{\mathrm{U}} = 8$ elements that is centered in the chamber and arranged in the horizontal plane. We evaluate the beamformer at N_{A} discrete values of the angle ϕ relative to the chamber center in this plane, with the nth angle $\phi_n = n\Delta\phi$ where $\Delta\phi = 2\pi/N_{\mathrm{A}}$. The PAS at ϕ_n can be expressed as

$$P(\phi_n) = |\mathbf{a}^{\dagger}(\phi_n)\mathbf{e}(\boldsymbol{\theta})|^2 \quad (2)$$

where the vector $\mathbf{e}(\boldsymbol{\theta})$ contains the field values at the UCA element locations that are a function of the RE phases contained in the vector $\boldsymbol{\theta}$, $\mathbf{a}$ is the array steering vector, and $\{\cdot\}^{\dagger}$ indicates a conjugate transpose. Our goal is to maximize the PAS at a certain angle ϕ_{n_0} relative to the PAS value in the sidelobes. We therefore use the fitness function

$$f(\boldsymbol{\theta}) = \frac{|\mathbf{a}^{\dagger}(\phi_{n_0})\mathbf{e}(\boldsymbol{\theta})|^2}{\frac{1}{N_{\mathrm{A}}-N_{\mathrm{B}}}\sum_n |\mathbf{a}^{\dagger}(\phi_n)\mathbf{e}(\boldsymbol{\theta})|^2} = \frac{P(\phi_{n_0})}{\frac{1}{N_{\mathrm{A}}-N_{\mathrm{B}}}\sum_n P(\phi_n)}, \quad (3)$$

where $n \notin [n_0 - N_{\mathrm{B}}/2, n_0 + N_{\mathrm{B}}/2]$ and N_{B} is the number of discrete angles that lie within the main lobe of the PAS. In this work we use $N_{\mathrm{A}} = 360$ and $N_{\mathrm{B}} = 80$. The denominator in (3) represents the average power spectrum in the sidelobe directions, as trials with different fitness functions reveals that using the gradient ascent algorithm with a fitness function based on average sidelobe level performs significantly better than it does with a fitness function based on the peak sidelobe level.

B. Gradient Ascent Algorithm

Our objective is to find the RE phases $\boldsymbol{\theta}$ that maximize the fitness function $f(\boldsymbol{\theta})$ in (3). The gradient ascent algorithm requires computation of the gradient $\nabla f(\boldsymbol{\theta})$ with respect to the phases of the REs. The ℓth element of this gradient is the derivative of $f(\boldsymbol{\theta})$ with respect to θ_ℓ, which can be expressed as

$$\frac{\partial f(\boldsymbol{\theta})}{\partial \theta_\ell} = \frac{P'_\ell(\phi_{n_0})\sum_n P(\phi_n) - P(\phi_{n_0})\sum_n P'_\ell(\phi_n)}{\frac{1}{N_{\mathrm{A}}-N_{\mathrm{B}}}\left[\sum_n P(\phi_n)\right]^2} \quad (4)$$

where

$$P'_\ell(\phi) = \frac{\partial}{\partial \theta_\ell}|\mathbf{a}^{\dagger}(\phi)\mathbf{e}(\boldsymbol{\theta})|^2 \quad (5)$$

$$= 2\mathrm{Re}\left\{\left[\mathbf{a}^{\mathrm{T}}(\phi)\mathbf{e}^*(\boldsymbol{\theta})\right]\left[\mathbf{a}^{\dagger}(\phi)\frac{\partial \mathbf{e}(\boldsymbol{\theta})}{\partial \theta_\ell}\right]\right\} \quad (6)$$

and $\{\cdot\}^*$ indicates a conjugate. Based on the results in [7], we can further write

$$\frac{\partial \mathbf{e}(\boldsymbol{\theta})}{\partial \theta_\ell} = je^{-j\theta_\ell}\mathbf{E}_{\mathrm{R}}^{\mathrm{T}}(\mathbf{\Gamma}^{-1} - \mathbf{S}_{\mathrm{RR}})^{-1}\mathbf{1}_{\ell\ell} \times (\mathbf{\Gamma}^{-1} - \mathbf{S}_{\mathrm{RR}})^{-1}\mathbf{S}_{\mathrm{RF}}\mathbf{a}_{\mathrm{F}} \quad (7)$$

where $\mathbf{E}_{\mathrm{R}}$ is a $N_{\mathrm{R}} \times N_{\mathrm{U}}$ matrix whose pth column represents $\mathbf{e}_{\mathrm{R}}(\mathbf{r})$ evaluated at the location of the pth element of the UCA and $\mathbf{1}_{\ell\ell}$ is the elementary matrix with all zeros except a one in the ℓth position on the main diagonal. Based on these results, the iterative update equation in the gradient ascent algorithm is given by

$$\boldsymbol{\theta}_{m+1} = \boldsymbol{\theta}_m + \delta\nabla f(\boldsymbol{\theta}), \quad (8)$$

where the subscript m is the iteration index and δ is the step size. We initially use $\delta = 5\times 10^{-3}$ and then adaptively change δ to improve convergence speed.

III. Results

We use the excitation vector $\mathbf{a}_{\mathrm{F}} = \mathbf{1}$ and initialize the gradient ascent algorithm with a random seed $\boldsymbol{\theta}_0$ whose elements are uniformly selected on the range $[0, 2\pi)$. We run the algorithm for $M = 1500$ iterations and store the final optimized RE phases $\boldsymbol{\theta}_M$. Since the final PAS quality depends on the selected main beam direction ϕ_{n_0}, we repeat the optimization for ϕ_{n_0} swept over the range $[0, \pi/2]$ (chosen based on the chamber symmetry). By repeating the optimization for N_{S} different random seeds and choosing the optimized result that maximizes the fitness function, we generally improve the quality of the solution. Figure 2 plots the mean sidelobe level (SLL) as a function of ϕ_{n_0}, where the mean is computed from $N_{\mathrm{I}} = 1000$ optimal solutions obtained using the gradient ascent algorithm with N_{S} random seeds per optimization run. The results show that even for $N_{\mathrm{S}} = 1$, the mean SLL is around -8 dB. Increasing N_{S} from 1 to 4 reduces the mean SLL to less than -11 dB. Generally, this demonstrates that

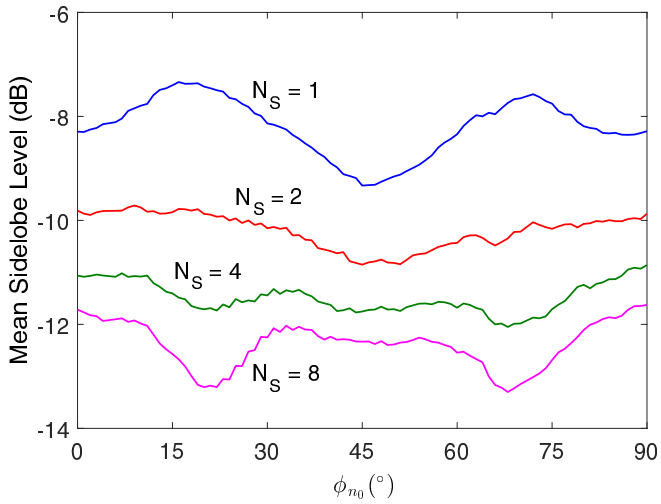

Fig. 2. Mean sidelobe level resulting from gradient ascent optimization as a function of the direction ϕ_{n_0} of the main beam for different numbers of random seeds.

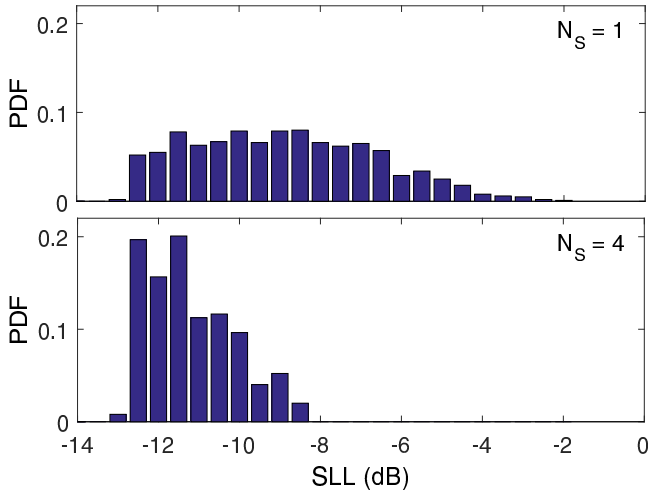

Fig. 3. Probability density function of the sidelobe level (SLL) when $\phi_{n_0} = 0^\circ$ for two different values of N_S.

using multiple random seeds quickly improves performance and that the gradient ascent algorithm is effective in finding reasonable solutions.

Figure 3 plots the probability density function (pdf) of the SLL when $\phi_{n_0} = 0$, highlighting the possible range in the achieved SLL over the N_I different optimizations. Comparing the two pdf plots for $N_S = 1$ and $N_S = 4$ reveals that a modest increase in N_S significantly reduces the likelihood of achieving a final solution with a high SLL. Figure 4 plots the PAS obtained for $\phi_{n_0} = 0^\circ$ and 45° with $N_S = 4$. The reasonable level of directionality in these results suggests that a simple gradient ascent based optimization employing multiple random realizations can be used for PAS optimization.

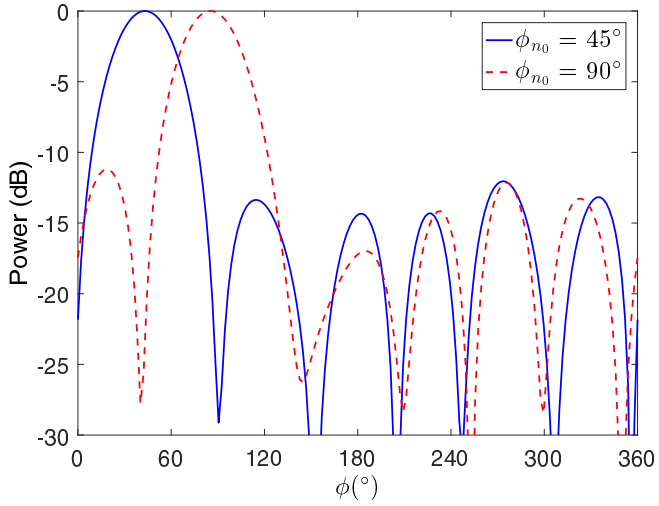

Fig. 4. Power angular spectrum (PAS) after optimization when $\phi_{n_0} = 45^\circ$ and 90° for $N_S = 4$.

IV. Conclusion

This paper demonstrates the use of a simple gradient ascent optimization algorithm for determining the reconfigurable impedance terminations to achieve a specified multipath field profile in a ROTAC. Simulation results based on full-wave FDTD analysis of the chamber coupled with network analysis to incorporate the impact of changing impedance states show that the optimization is able to provide RE impedance states that produce reasonably directive results at the device under test. Future work will focus on using alternate initialization techniques for the search as well as exploring the impact of practical constraints, such as loss and limited phase tuning range, of the reconfigurable impedances.

References

[1] W. Fan, X. Carreño Bautista de Lisbona, F. Sun, J. Ø Nielsen, M. B. Knudsen, and G. F. Pedersen, "Emulating spatial characteristics of MIMO channels for OTA testing," *IEEE Transactions on Antennas and Propagation*, vol. 61, no. 8, pp. 4306–4314, Aug. 2013.

[2] P. Kyösti, J. P. Nuutinen, and T. Jämsä, "MIMO OTA test concept with experimental and simulated verification," in *Proc. 4th European Conference on Antennas and Propagation*, Apr. 2010.

[3] M. A. Garcia-Fernandez, J. D. Sanchez-Heredia, A. M. Martinez-Gonzalez, D. A. Sanchez-Hernandez, and J. F. Valenzuela-Valdes, "Advances in mode-stirred reverberation chambers for wireless communication performance evaluation," *IEEE Communications Magazine*, vol. 49, no. 7, pp. 140–147, July 2011.

[4] R. Mehmood, J. W. Wallace, and M. A. Jensen, "Reconfigurable OTA chamber for MIMO wireless device testing," in *Proc. 10th European Conference on Antennas and Propagation*, Apr. 2016.

[5] J. W. Wallace, R. Mehmood, and M. A. Jensen, "Electronically reconfigurable reverberation chambers," in *Proc. 8th European Conference on Antennas and Propagation*, Apr. 2014, pp. 3669–3673.

[6] R. Mehmood, J. W. Wallace, and M. A. Jensen, "PAS control in a reconfigurable OTA chamber," in *Proc. IEEE International Symposium on Antennas and Propagation*, July 2015, pp. 292–293.

[7] P. Baniya, S. Ur Rehman, and J. W. Wallace, "Efficient optimization of reconfigurable parasitic antenna arrays using geometrical considerations," in *Proc. 5th European Conference on Antennas and Propagation*, Apr. 2011, pp. 270–274.